AJNR

MR Angiography at 3T versus Digital Subtraction Angiography in the Follow-up of Intracranial Aneurysms Treated with Detachable Coils

Charles B. L. M. Majoie, Marieke E. Sprengers, Willem Jan J. van Rooij, Cristina Lavini, Menno Sluzewski, Jeroen C. van Rijn and Gerard J. den Heeten

AJNR Am J Neuroradiol 2005, 26 (6) 1349-1356
http://www.ajnr.org/content/26/6/1349

AJNR Am J Neuroradiol 26:1349–1356, June/July 2005

MR Angiography at 3T versus Digital Subtraction Angiography in the Follow-up of Intracranial Aneurysms Treated with Detachable Coils

Charles B. L. M. Majoie, Marieke E. Sprengers, Willem Jan J. van Rooij, Cristina Lavini, Menno Sluzewski, Jeroen C. van Rijn, and Gerard J. den Heeten

BACKGROUND AND PURPOSE: **Digital subtraction angiography (DSA) is used to follow-up intracranial aneurysms treated with detachable coils to identify recurrence and determine need for additional treatment. However, DSA is invasive and involves a small risk of neurologic complications. We assessed the feasibility and usefulness of 3D time-of-flight (TOF) MR angiography (MRA) performed at 3T compared with DSA for the follow-up of coil-treated intracranial aneurysms.**

METHODS: **In a prospective study, 20 consecutive patients with 21 intracranial aneurysms treated with coils underwent DSA and nonenhanced and enhanced multiple overlapping thin-slab acquisition 3D TOF MRA at 3T on the same day at a mean follow-up of 6 months (range, 4–14 months) after coil placement. MRA images were evaluated for presence of artifacts, presence and size of aneurysm remnants and recurrences, patency of parent and branch vessels, and added value of contrast material enhancement. MRA and DSA findings were compared.**

RESULTS: **Interobserver agreement of MRA was good, as was agreement between MRA and DSA. All three recurrences that needed additional treatment were detected with MRA. Minor disagreement occurred in four cases: three coil-treated aneurysms were scored on MRA images as having a small remnant, whereas on DSA images these aneurysms were occluded; the other aneurysm was scored on MRA images as having a small remnant, whereas on DSA images this was a small recurrence. Use of contrast material had no additional value. Coil-related MR imaging artifacts were minimal and did not interfere with evaluation of the occlusion status of the aneurysm.**

CONCLUSION: **High-spatial-resolution 3D TOF MRA at 3T is feasible and useful in the follow-up of patients with intracranial aneurysms treated with coil placement.**

Endovascular treatment with detachable coils has become an established technique for patients with intracranial aneurysms (1). In 14–33% of cases, the aneurysm may partially recur due to coil compaction or enlargement of a remnant, depending on the original size of the aneurysm, initial occlusion rate, and length of follow-up (2–6). Therefore, all patients with coil-treated intracranial aneurysms are followed up with digital subtraction angiography (DSA) to identify aneurysm recurrence and to determine the subsequent need for additional endovascular or surgical treatment. DSA is, however, an invasive imaging technique that involves a small but significant risk of neurologic complications, estimated to occur in 0.3–1.8% of cases (7, 8).

Previous *in vitro* studies have demonstrated that detachable coils are compatible with MR imaging in terms of safety and image quality at both 1.5 T (9, 10) and 3T (11, 12). MR angiography (MRA) is a safe and noninvasive imaging technique that has become a realistic diagnostic option for the follow-up of intracranial aneurysms treated with coils (13), as demonstrated in previous studies performed on MR units with field strengths of 1.0 or 1.5 T (14–23). Some of

Received September 1, 2004; accepted after revision October 26.

From the Departments of Radiology (C.B.L.M.M., M.E.S., W.J.J.v.R., C.L., G.J.d.H.), and Biostatistics (J.C.R.), Academic Medical Center, University of Amsterdam, and the Department of Radiology (W.J.J.v.R., M.S.) St. Elisabeth Ziekenhuis, Hilvarenbeekseweg, the Netherlands.

Address reprint requests to Charles B. L. M. Majoie, MD, PhD, Department of Radiology, Academic Medical Center, University of Amsterdam, PO Box 22660, 1100 DD Amsterdam, the Netherlands.

these studies advocate the use of contrast material-enhanced MRA to increase sensitivity for detection of residual flow (18, 20, 22). MRA at 3T provides images with higher spatial resolution than that of MRA at 1.5 T (24–26), and improvement of sensitivity to detect aneurysm remnants or recurrences is to be expected.

The purpose of our study was to prospectively assess the feasibility and usefulness of MRA, including nonenhanced and contrast-enhanced multiple overlapping thin slab acquisition (MOTSA) 3D time-of-flight (TOF) MRA performed at 3T as compared with DSA for the follow-up of aneurysms treated with detachable coils.

Methods

Patients

Between November 2003 and July 2004, 20 consecutive patients (nine men, 11 women; age range, 18–74 years; mean age, 49 years) with 21 aneurysms (20 ruptured, one unruptured) underwent DSA and MR imaging on the same day, at a mean follow-up period of 6 months (range, 4–14 months) after endovascular treatment with detachable coils (Guglielmi detachable coils; Boston Scientific, Freemont, CA). The local ethics committee approved the study, and written informed consent was obtained from all patients. The locations of the aneurysms were as follows: anterior communicating artery (n = 6), posterior communicating artery (n = 5), middle cerebral artery (n = 2), internal carotid artery (n = 1), basilar tip (n = 3), posterior inferior cerebellar artery (n = 2), superior cerebellar artery (n = 1), and anterior inferior cerebellar artery (n = 1). The size of the aneurysms was 5 mm or less in six cases, 6–10 mm in 11, and more than 10 mm in four.

MR Imaging Techniques

All MR examinations were performed with a 3T system (Intera R10; Philips Medical Systems, Best, the Netherlands) by using the sensitivity encoding (SENSE) phased-array head coil (MRI Devices; Gainesville, FL). All patients underwent the same MR imaging protocol that included axial T2-weighted fast spin-echo, nonenhanced and enhanced axial T1-weighted spin-echo, and MOTSA 3D TOF MRA sequences. Imaging parameters for the T1-weighted spin-echo sequence were 570/12 (TR/TE), 256 × 256 matrix (reconstructed to 512 × 512), 180-mm FOV, 90% rectangular FOV, 3-mm thick sections with a 0.3-mm gap. Parameters for the T2-weighted fast spin-echo sequence were 3394/80, 400 × 400 matrix (reconstructed to 512 × 512), 230-mm FOV, 70% rectangular FOV, 5-mm thick sections with a 0.5-mm gap. The volume of the MOTSA 3D TOF MRA was localized on a sagittal 2D phase-contrast scout image. A presaturation band was applied above the imaging volume to saturate incoming venous blood. For the MOTSA 3D TOF MRA sequence, the parameters were as follows: 3D fast field echo T1-weighted sequence, 21/4, flip angle 20°, 512 × 512 matrix (reconstructed to 1024 × 1024), 200-mm FOV, 85% rectangular FOV, 1.0-mm-thick sections interpolated to 0.5 mm, 160 sections acquired in eight chunks. The measured voxel size of the MOTSA 3D TOF MRA image was 0.39 × 0.61 × 1 mm, and the reconstructed voxel size was 0.2 × 0.2 × 0.5 mm. Imaging time of the high-spatial-resolution MOTSA 3D TOF sequence was reduced by parallel imaging. For parallel imaging, we used SENSE, a technique that uses multiple coil elements to encode spatial information in addition to traditional gradient encoding. Less gradient encodings are required, resulting in shorter imaging times (27). By using the SENSE head coil with a SENSE reduction factor of 1.5, we could limit the acquisition time to 7 minutes 14 seconds. Tilted optimized nonsaturating excitation was used in this protocol to optimize excitation profiles (3).

After the intravenous administration of 0.2 mL of gadopentetate dimeglumine (Magnevist; Schering AG, Berlin, Germany) per kilogram of bodyweight, the MOTSA 3D TOF MRA and axial T1-weighted spin-echo sequences were repeated. The T1- and T2-weighted images were obtained to evaluate the degree to which coils produce artifacts at 3T. Also, the T1-weighted spin-echo images were obtained to detect T1 shortening due to thrombus that may occasionally be interpreted as residual flow within the aneurysm on the MRA image. Total examination time for MR imaging was 45 minutes.

DSA Technique

DSA was performed after the MR examination on the same day with a single-plane angiographic unit (Integris Allura Neuro; Philips Medical Systems). Six to eight milliliters of nonionic contrast material (iodixanol, Visipaque 320 mgI/mL; Amersham Health, Cork, Ireland) was injected into the internal carotid or vertebral artery with a power injector at 4–6 mL/s. Three views were acquired in each patient, including the view that showed the aneurysm best at the time of embolization. Three-dimensional angiography was performed before endovascular treatment but was not performed for follow-up. Complications of angiography were recorded.

Image Analysis

Findings at follow-up DSA were classified by two neuroradiologists (C.B.L.M.M., M.S.) in consensus, in conjunction with the pretreatment DSA and the DSA performed during the coiling procedure. A remnant was defined as residual aneurysm filling (including a neck remnant, dog ear, or residual filling in the aneurysm sac) present on the DSA image immediately after coil placement. It was also called a remnant at the follow-up study if it did not increase in size. An aneurysm recurrence was defined as filling of the aneurysm at the follow-up study that was not present on the DSA image obtained immediately after coil placement or as an enlargement of a remnant.

Two observers (M.E.S., W.J.J.R.), blinded to follow-up DSA images, assessed MR images independently, together with the pretreatment DSA images and the DSA images obtained during the coiling procedure. Source images and multiple maximum intensity projections of MRA images were both used. MR images were evaluated for artifacts, presence and size of aneurysm remnants and recurrences, patency of parent and branch vessels, and added value of contrast material enhancement. The contrast-enhanced MRA images were scored separately from the nonenhanced images with an interval of 2 months. These were also evaluated for the presence of venous overlap. For MRA, sizes of aneurysm remnants or recurrences were directly measured on a workstation, and for DSA these sizes were estimated by comparison with the diameter of the internal carotid or basilar artery. Interobserver variability was assessed with κ statistics. After the blinded study, discrepancies were resolved by consensus. Finally, the consensus data of the MRA images were compared with DSA findings.

Results

MRA and DSA images were of sufficient quality in all patients. One patient had a transient visual deficit related to DSA; there were no complications from MRA.

Interobserver agreement for the identification of aneurysm occlusion, remnant, or recurrence with use of MRA was good (κ = 0.77; 95% confidence interval [CI]: 0.54–1.0), with a full agreement in 18 (86%) of 21 aneurysms. Disagreement occurred in three cases:

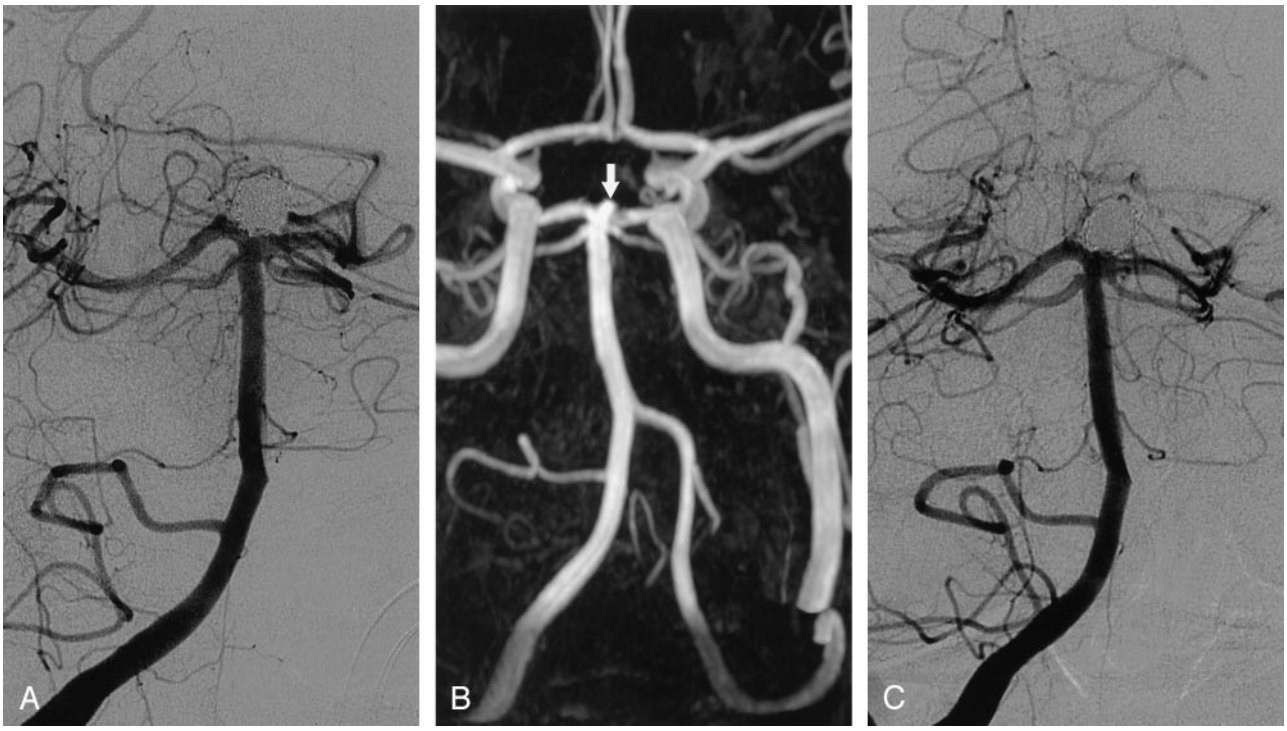

FIG 1. Interobserver disagreement on MRA and disagreement between MRA and DSA on the occlusion of a basilar tip aneurysm after treatment with coils.

A, DSA image obtained immediately after treatment with coils shows complete aneurysm occlusion.

B, Nonenhanced MOTSA 3D TOF MRA image obtained 5 months after treatment shows filling of the aneurysm neck (arrow), which was interpreted by one observer as a 2-mm remnant and by the other observer as a 2-mm recurrence. During the consensus reading, it was scored as a remnant. Note minor signal intensity loss in the proximal P1 segment of the left posterior cerebral artery.

C, DSA image obtained 5 months after treatment with coils. This image was interpreted as occlusion.

Results of MRA at 3.0 T versus DSA in 21 intracranial aneurysms after treatment with detachable coils

	DSA			
MRA	Recurrence	Remnant	Occlusion	Total
Recurrence	3	0	0	3
Remnant	1*	5	3	9
Occlusion	0	0	9	9
Total	4	5	12	21

Note—κ = 0.70 (95% CI: 0.44–0.95); full agreement = 81% (17/21)

* Coil-treated aneurysm was scored as a 2-mm recurrence on DSA image, and as a 2-mm remnant on MRA images. Additional treatment was not required.

one observer interpreted three coil-treated aneurysms as having a 2-mm remnant, whereas the other observer judged these as occluded in two and as a 2-mm recurrence in one (Fig 1). Correlation between MRA and DSA was good (κ = 0.70; 95% CI: 0.44–0.95), with full agreement in 17 (81%) of 21 aneurysms (Table), including nine occlusions, five remnants (Fig 2), and three recurrences (Figs 3 and 4). Of the five remnants, four measured 3 mm or less and one measured 5 mm. Of the three recurrences, two measured 4 mm and one measured 6 mm. The three recurrences were additionally treated with coiling in two and clipping in one. Disagreement between MRA and DSA occurred in four cases: three coiled aneurysms were scored on MRA image as having a 2-mm remnant, whereas on DSA images these were judged as occluded (Fig 1). Another aneurysm was scored on MRA images as having a 2-mm remnant, whereas on DSA images this was scored as a 2-mm recurrence (including a 1-mm remnant) due to minor coil compaction (Fig 5). This small recurrence did not require additional treatment.

Enhancement of venous structures was present on all contrast-enhanced 3D TOF MRA images, but venous overlap did not interfere with image interpretation. The use of contrast material provided no additional value to the evaluation of occlusion status of the coil-treated aneurysms (Fig 3), nor to the evaluation of parent or branch vessel patency (Fig 6).

A high-signal-intensity rim artifact was present on T1- and T2-weighted MR images around 16 (76%) of 21 coil-treated aneurysms (Fig 3A) and around three aneurysms (14%) on MRA images. This rim artifact was less pronounced on the MRA images than on the T1- and T2-weighted images and did not interfere with interpretation of the occlusion status of the aneurysms. On the 3D TOF axial source images, the high-signal-intensity rim was not observed at the neck area. A large high-signal-intensity area due to clot-containing methemoglobin was observed on the T1-weighted and MRA images in one giant, partially thrombosed posterior inferior cerebellar artery aneurysm. This was, however, not present at the neck area and did not influence the evaluation of the occlusion

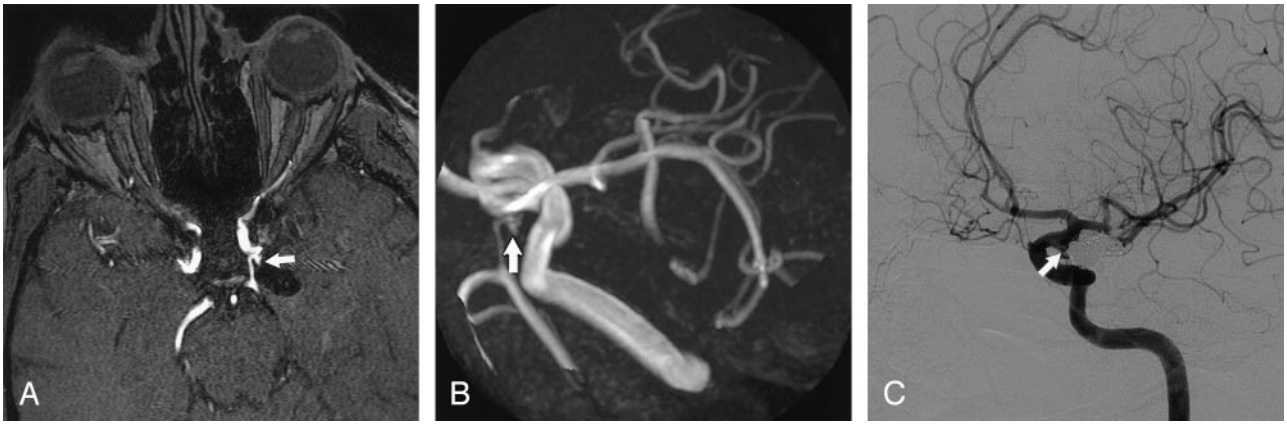

FIG 2. Posterior communicating artery aneurysm with small neck remnant 7 months after treatment with coils.
A, Axial nonenhanced MOTSA 3D TOF MRA source image demonstrates a 2-mm neck remnant (arrow).
B, Nonenhanced MOTSA 3D TOF MR target maximum intensity projection image also shows a small neck remnant (arrow).
C, DSA image confirms the presence of a small neck remnant (arrow).

status. Coil-related signal intensity loss mimicking narrowing of parent or branch vessels was observed in seven (33%) of 21 aneurysms, both on nonenhanced and contrast-enhanced MRA images, but it did not prevent evaluation of the aneurysm neck (Figs 1 and 6). These seven aneurysms included three anterior communicating artery aneurysms, one posterior communicating artery aneurysm, one middle cerebral artery aneurysm, one basilar tip aneurysm, and one superior cerebellar artery aneurysm. Artifactual occlusions of parent or branch vessels were not observed.

Discussion

We found good interobserver agreement with 3T MRA and good agreement between 3T MRA and DSA in the evaluation of occlusion status in the follow-up of coil-treated aneurysms. One small recurrence due to coil compaction was interpreted as a remnant on MRA images: subtle changes in the coil mesh configuration that indicate compaction are more easily appreciated on (nonsubtracted) DSA images. MRA showed three 2-mm remnants, not demonstrated with DSA. The detection of these small remnants may be attributed to the high spatial resolution of our MOTSA 3D TOF MRA technique at 3T and to the fact that follow-up DSA was performed in three projections, whereas with MRA any projection was available. These small remnants may have been obscured by the overlying coil mesh on the DSA projections. We did not perform 3D angiography for the follow-up of coil-treated cerebral aneurysms since the large difference in density between the platinum coils and the contrast agent in the vessels precludes tresholding the 3D dataset in a way that both the coil mesh and the vessels are visualized simultaneously. One may argue that knowledge of the findings of pretreatment DSA and of DSA performed immediately after the coil procedure might have influenced the interpretation of the MRA images in the present study. We, however, believe that this method of image analysis resembles that in clinical practice and was, therefore, justified.

MRA at 1.0 T and 1.5 T has been shown to be useful in assessing the occlusion status of aneurysms treated with detachable coils (14–23). In most of these studies, remnants and recurrences are combined as residual flow. Sensitivity of 1.0-T and 1.5-T MRA ranges from 60% to 100% and specificity from 90% to 100% (14–23). MRA at a higher field strength results in a more efficient suppression of the background tissue as the T1 longitudinal relaxation time (on which the magnetic labeling is based) is longer (24–26, 28). The higher field strength also provides better signal-to-noise ratio, which is beneficial for detecting and resolving small vessels, aneurysm remnants, and recurrences. The use of small voxels reduces intravoxel dephasing (29). Our study was limited to the evaluation of MRA at 3T compared with DSA. Therefore, we cannot draw any conclusion with respect to the added value of MRA at 3T compared with MRA at 1.0 or 1.5 T.

In general, sensitivity of MRA is limited by flow saturation caused by turbulent or slow flow in aneurysm remnants. These saturation effects may be reduced by the use of the MOTSA 3D TOF technique instead of a single-volume 3D TOF sequence (29, 30). MOTSA 3D TOF MRA minimizes signal intensity loss due to spin saturation, maintains small voxels and short TEs to minimize intravoxel phase dispersion (29), and allows larger imaging volumes. With MOTSA 3D TOF MRA at 3T, we were able to reconstruct a voxel size of $0.2 \times 0.2 \times 0.5$ mm, and aneurysm remnants and recurrences smaller than 3 mm could be detected.

Contrast Material Enhancement

Contrast enhancement may reduce saturation effects on 3D TOF MRA and dynamic ultrafast MRA images (18, 20, 22, 23, 30–32), improving the visual-

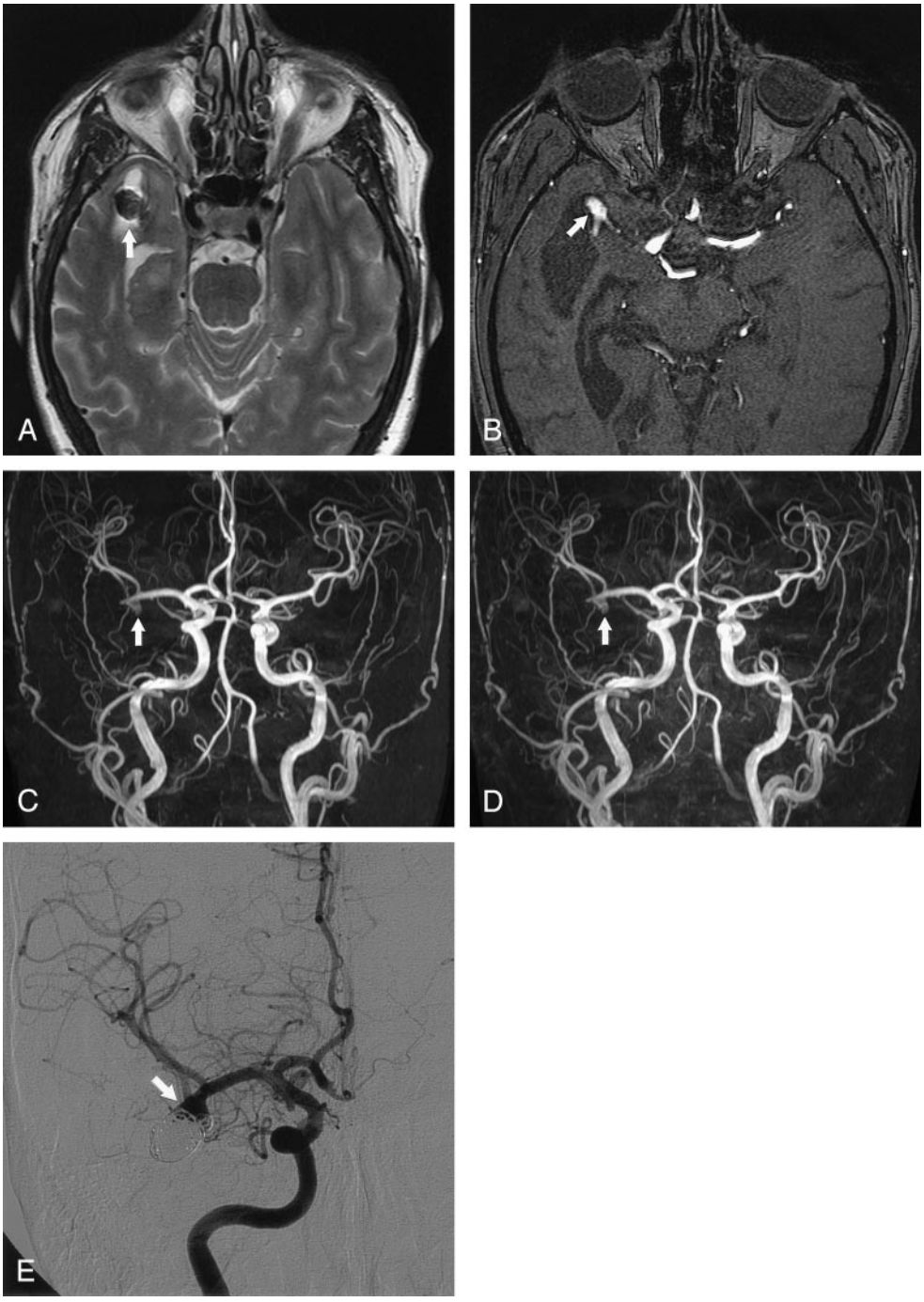

FIG 3. Middle cerebral artery aneurysm with high-signal-intensity rim artifact and recurrence 6 months after treatment with detachable coils.

A, Axial fast spin-echo T2-weighted MR image (3394/80) shows a 2-mm rim of increased signal intensity around the coils (arrow).

B, Axial nonenhanced MOTSA 3D TOF MRA source image demonstrates recurrence of the aneurysm (arrow).

C, Nonenhanced MOTSA 3D TOF MRA image shows recurrence (arrow).

D, Contrast-enhanced MOTSA 3D TOF MRA image shows the same recurrence (arrow).

E, DSA image obtained 6 months after treatment confirms the presence of recurrence (arrow).

ization of giant aneurysms (32) and large remnants or recurrences of aneurysms treated with coils (18).

Contrast-enhanced 3D TOF MRA also benefits from imaging at 3T. T1 shortening in enhanced blood combined with T1 lengthening due to increased field strength in background tissues improves blood-to-background contrast (33). However, the use of intravenous contrast material had no additional value in the current study. Saturation reduction by the use of the MOTSA technique and the absence of large remnants or recurrences in our relatively small study of 21 aneurysms may explain the lack of added value of contrast material administration.

Coil-Related Artifacts

The platinum coil wires can produce susceptibility artifacts, although previous studies found a relative lack of susceptibility effects of coils *in vitro* and *in vivo* at 1.5 T (9, 10, 14). At higher field strength, increased susceptibility artifacts from paramagnetic substances are expected. In an *in vitro* study of MR compatibility of detachable coils at 3T, however, only minor susceptibility artifacts were found in the readout direction on gradient-echo images (11). Magnetic field mapping showed no induced field inhomogeneity (11). Also, no change in temperature was measured

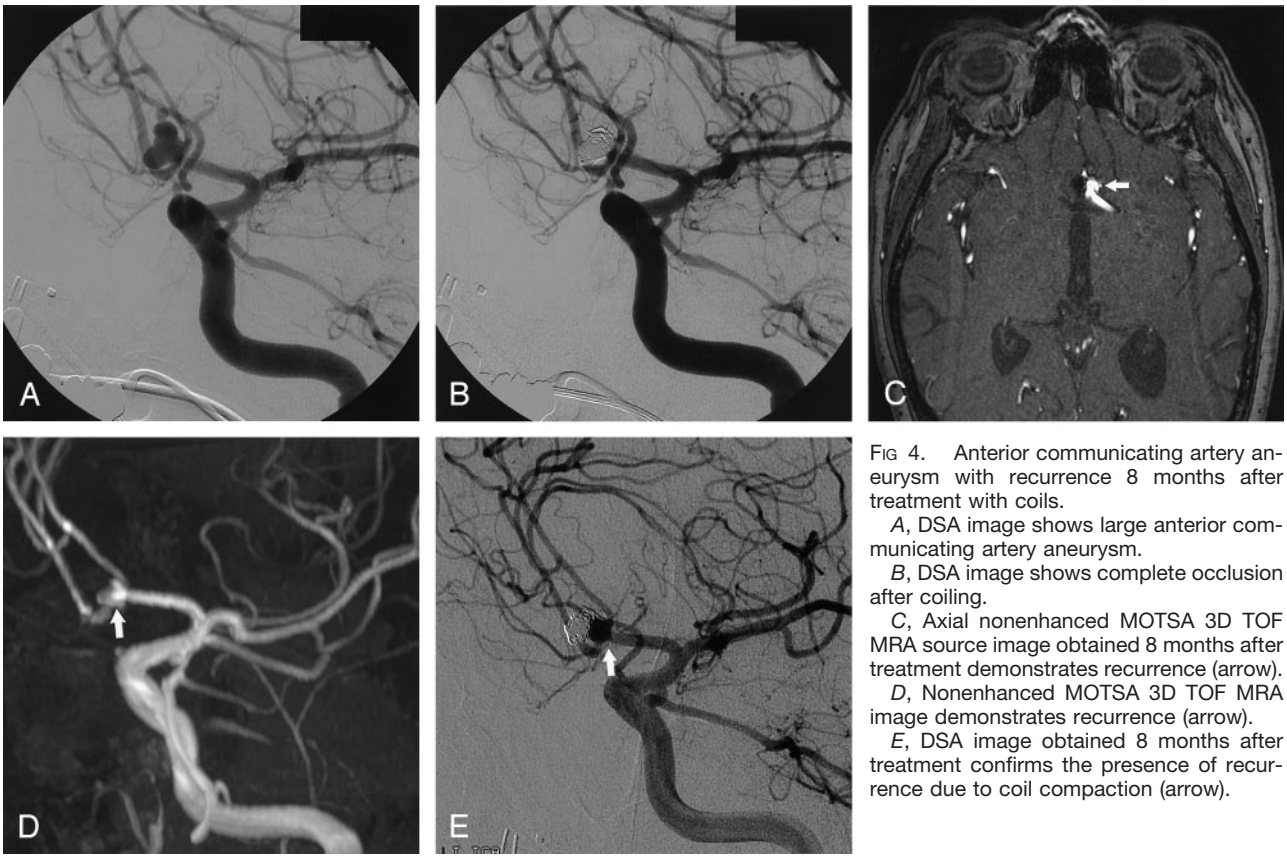

FIG 4. Anterior communicating artery aneurysm with recurrence 8 months after treatment with coils.

A, DSA image shows large anterior communicating artery aneurysm.

B, DSA image shows complete occlusion after coiling.

C, Axial nonenhanced MOTSA 3D TOF MRA source image obtained 8 months after treatment demonstrates recurrence (arrow).

D, Nonenhanced MOTSA 3D TOF MRA image demonstrates recurrence (arrow).

E, DSA image obtained 8 months after treatment confirms the presence of recurrence due to coil compaction (arrow).

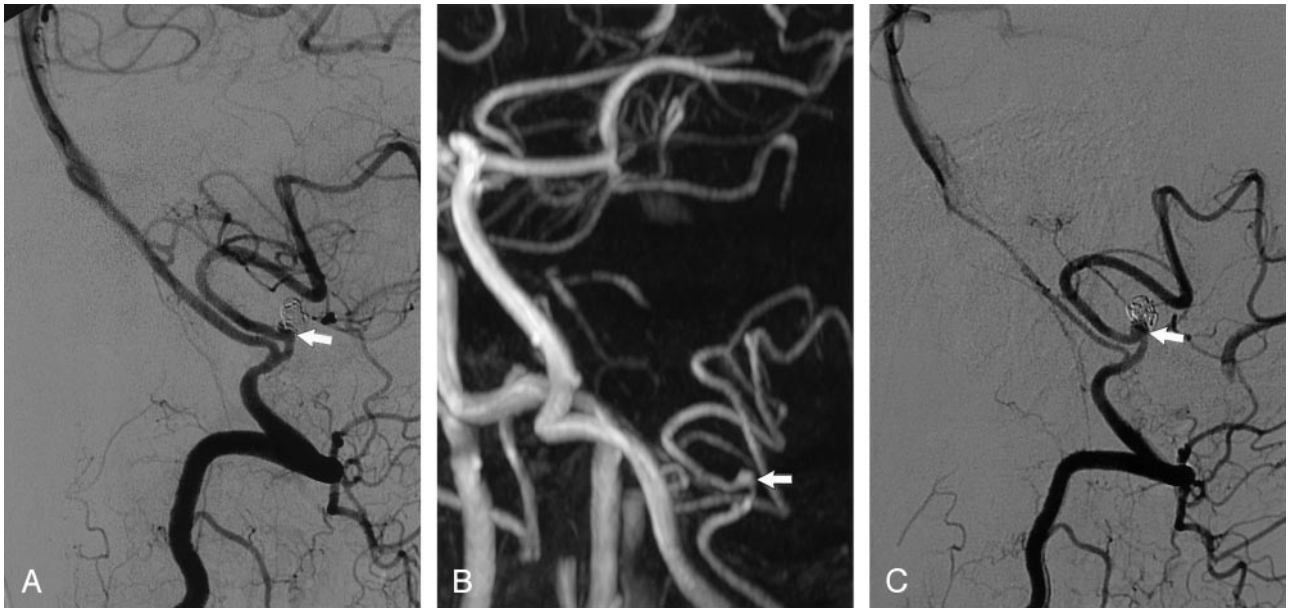

FIG 5. Disagreement between MRA and DSA on the occlusion status of a posterior inferior cerebellar artery aneurysm 14 months after treatment with coils.

A, DSA image obtained immediately after coiling shows a small area of residual filling (arrow).

B, Nonenhanced MOTSA 3D TOF MRA image obtained 14 months after treatment shows flow in the aneurysm neck (arrow), which was interpreted as a 2-mm remnant by both observers.

C, DSA image shows filling of the aneurysm neck (arrow), which was interpreted as a 2-mm recurrence (including a 1-mm remnant) due to coil compaction. Both observers thought that additional treatment for this small recurrence was not indicated.

during movement into the imager bore or within the bore, and no evidence of deflection of the coil mass was found (24). At 3T, we found a high-signal-intensity rim artifact on T1-weighted spin-echo and T2-weighted fast spin-echo images around the coil mesh in most aneurysms, but on MRA images around only

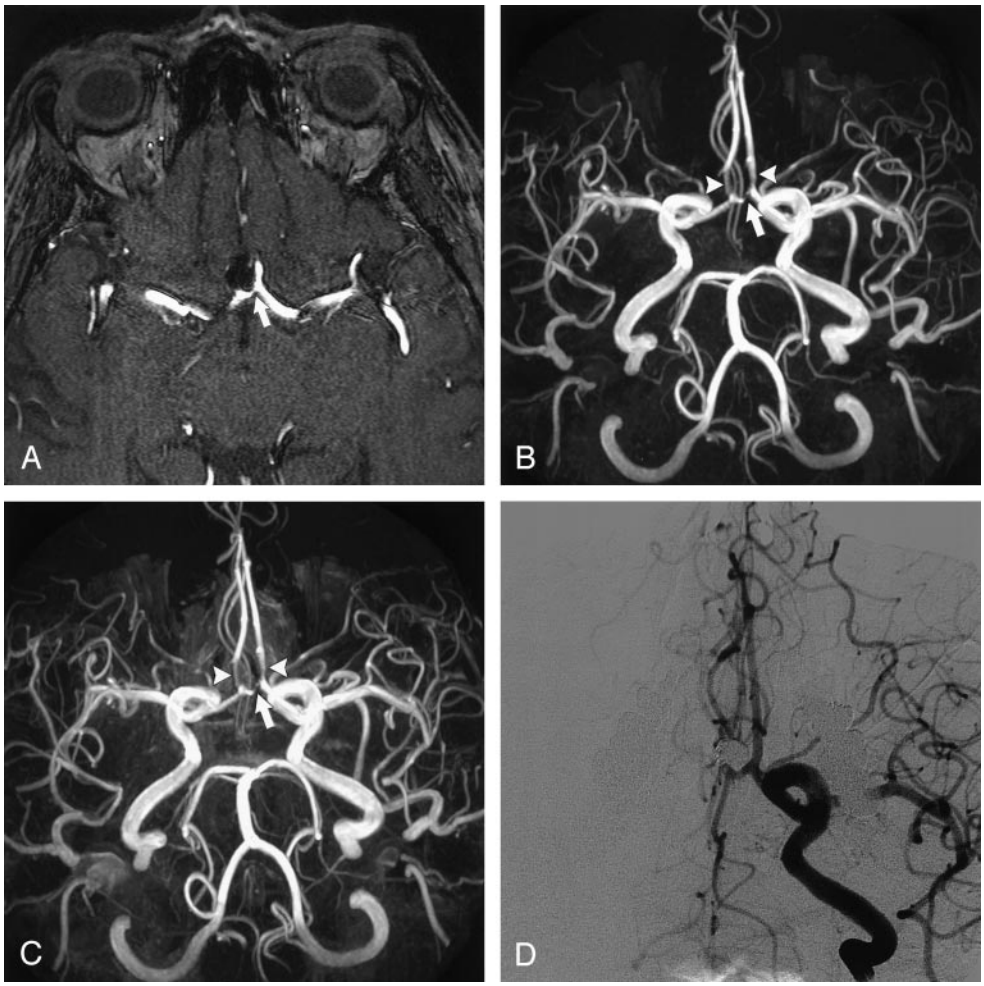

FIG 6. Anterior communicating artery aneurysm with coil-related signal intensity loss in parent and branch vessels.
A, Axial nonenhanced MOTSA 3D TOF MRA source image obtained 8 months after treatment shows narrowing of the anterior communicating artery (arrow). No neck remnant or aneurysm recurrence was found.
B, Nonenhanced MOTSA 3D TOF MRA image shows narrowing of the anterior communicating artery (arrow) and the proximal part of both A2 segments of the anterior cerebral arteries (arrowheads).
C, Enhanced MOTSA 3D TOF MRA image shows similar narrowings as described in *B*.
D, DSA image shows complete occlusion of the aneurysm without narrowing of parent and branch vessels.

three aneurysms. This artifact did not interfere with interpretation of the occlusion status because the high-signal-intensity rim was not observed on the 3D TOF axial source images at the neck area.

Coil-induced signal intensity loss mimicking parent and branch vessel narrowing or occlusion has been described previously on 3D TOF MRA images (16–18). This signal intensity loss may prevent evaluation of the parent artery and aneurysm neck in up to 11% of cases on 1.5-T images (18). Although this artifact was observed in seven (33%) of 21 coil-treated aneurysms in our study, it was not so severe as to prevent evaluation of the aneurysm neck.

Conclusion

MOTSA 3D TOF MRA at 3T is feasible and useful in the follow-up of patients with intracranial aneurysms treated with coil placement. Aneurysm recurrences and remnants are depicted accurately. Imaging artifacts are minimal. The use of intravenous contrast material provided no additional value. MRA might become the primary imaging method for the follow-up of coil-treated aneurysms. Larger studies are warranted to validate these conclusions and to evaluate the added value of MRA techniques at 3T compared with those performed at lower field strength.

References

1. Molyneux A, Kerr R, Stratton I, et al, International Subarachnoid Aneurysm Trial (ISAT) Collaborative Group. **International Subarachnoid Aneurysm Trial (ISAT) of neurosurgical clipping versus endovascular coiling in 2143 patients with ruptured intracranial aneurysms: a randomised trial.** *Lancet* 2002;360:1267–1274
2. Cognard C, Weill A, Spelle L, et al. **Long-term angiographic follow-up of 169 intracranial aneurysms occluded with detachable coils.** *Radiology* 1999;212:348–356
3. Thornton J, Debrun GM, Aletich VA, Bashir Q, Charbel FT, Ausman JI. **Follow-up angiography of intracranial aneurysms treated with endovascular placement of Guglielmi detachable coils.** *Neurosurgery* 2002;50:239–249
4. Sluzewski M, van Rooij WJ, Rinkel GJE, Wijnalda D. **Endovascular treatment of ruptured intracranial aneurysms with detachable coils: long-term clinical and serial angiographic results.** *Radiology* 2003;227:720–724

5. Raymond J, Guilbert F, Weill A, et al. **Long-term angiographic recurrences after selective endovascular treatment of aneurysms with detachable coils.** *Stroke* 2003;34:1398–1403
6. Sluzewski M, van Rooij WJ, Slob MJ, Bescós JO, Slump CH, Wijnalda D. **Relation between aneurysm volume, packing, and compaction in 145 cerebral aneurysms treated with coils.** *Radiology* 2004;231:653–658
7. Cloft HJ, Joseph GJ, Dion JE. **Risk of cerebral angiography in patients with subarachnoid hemorrhage, cerebral aneurysm and arteriovenous malformation: a meta-analysis.** *Stroke* 1999;30:317–320
8. Willinsky RA, Taylor SM, terBrugge K, Farb RI, Tomlinson G, Montanera W. **Neurologic complications of cerebral angiography: prospective analysis of 2899 procedures and review of the literature.** *Radiology* 2003;227:522–528
9. Hartman J, Nguyen T, Larsen D, Teitelbaum P. **MR artifact, heat production, and ferromagnetism of Guglielmi detachable coils.** *AJNR Am J Neuroradiol* 1997;18:497–501
10. Shellock FG, Detrick MS, Brant-Zawadzki M. **MR compatibility of Guglielmi detachable coils.** *Radiology* 1997;203:568–570
11. Hennemeyer CT, Wicklow K, Feinberg DA, Derdeyn CP. **In vitro evaluation of platinum Guglielmi detachable coils at 3 T with a porcine model: safety issues and artifacts.** *Radiology* 2001;219:732–737
12. Shellock FG. **Biomedical implants and devices: assessment of magnetic field interactions with a 3.0-Tesla MR system.** *J Magn Reson Imaging* 2002;16:721–732
13. Summers PE, Jarosz JM, Markus H. **MR angiography in cerebrovascular disease.** *Clin Radiol* 2001;56:437–456
14. Derdeyn CP, Graves VB, Turski PA, Masaryk AM, Strother CM. **MR angiography of saccular aneurysm after treatment with Guglielmi detachable coils: preliminary experience.** *AJNR Am J Neuroradiol* 1997;18:279–286
15. Gonner F, Heid L, Remonda G, et al. **Angiography with ultrashort echo times in cerebral aneurysms treated with Guglielmi detachable coils.** *AJNR Am J Neuroradiol* 1998;19:1324–1328
16. Brunereau L, Cottier JP, Sonier CB, et al. **Prospective evaluation of time-of-flight MR angiography in the follow-up of intracranial saccular aneurysms treated with Guglielmi detachable coils.** *J Comput Assist Tomogr* 1999;23:216–223
17. Kähära VJ, Seppänen SK, Ryymin PS, Mattila P, Kuurne T, Laasonen EM. **MR angiography with three-dimensional time-of-flight and targeted maximum-intensity-projection reconstructions in the follow-up of intracranial aneurysms embolized with Guglielmi detachable coils.** *AJNR Am J Neuroradiol* 1999;20:1470–1475
18. Anzalone N, Righi C, Simionato F, et al. **Three dimensional time-of-flight MR angiography in the evaluation of intracranial aneurysms treated with Guglielmi detachable coils.** *AJNR Am J Neuroradiol* 2000;21:746–752
19. Weber W, Yousry TA, Felber SR, et al. **Noninvasive follow-up of GDC-treated saccular aneurysms by MR angiography.** *Eur Radiol* 2001;11:1792–1797
20. Boulin A, Pierot L. **Follow-up of intracranial aneurysms treated with detachable coils: comparison of gadolinium-enhanced 3D time-of-flight MR angiography and digital subtraction angiography.** *Radiology* 2001;219:108–113
21. Nome T, Bakke SJ, Nakstad PH. **MR angiography in the follow-up of coiled aneurysms after treatment with Guglielmi detachable coils.** *Acta Radiol* 2002;43:10–14
22. Leclerc X, Navez JF, Gauvrit JY, Lejeune JP, Pruvo JP. **Aneurysms of the anterior communicating artery treated with Guglielmi detachable coils: follow-up with contrast-enhanced MR angiography.** *AJNR Am J Neuroradiol* 2002;23:1121–1127
23. Cottier JP, Bleuzen-Couthon AB, Gallas S, et al. **Intracranial aneurysms treated with Guglielmi detachable coils: is contrast material necessary in the follow-up with 3D time-of-flight MR angiography?** *AJNR Am J Neuroradiol* 2003;24:1797–1803
24. Bernstein MA, Huston J III, Lin C, Gibbs GF, Felmlee JP. **High-resolution intracranial and cervical MRA at 3T: technical considerations and initial experience.** *Magn Reson Med* 2001;46:955–962
25. AL-Kwifi O, Emery DJ, Wilman AH. **Vessel contrast at 3 Tesla in time-of-flight magnetic resonance angiography of the intracranial and carotid arteries.** *J Magn Reson Imaging* 2002;20:181–187
26. Gibbs GF, Huston J III, Bernstein MA, Riederer SJ, Brown RD. **Improved image quality of intracranial aneurysms: 3T versus 1.5-T time-of-flight MR angiography.** *AJNR Am J Neuroradiol* 2004;25:84–87
27. Pruessmann KP, Weiger W, Scheidegger MB, Boesiger P. **SENSE: sensitivity encoding for fast MRI.** *Magn Res Med* 1999;42:952–962
28. Wansapura J, Holland S, Dunn R, Ball W. **NMR relaxation times at 3 tesla.** *J Magn Reson Imag* 1999;9:531–538
29. Davis WL, Warnock SH, Harnsberger HR, Parker DL, Chen CX. **Intracranial MRA: single volume vs. multiple thin slab 3D time-of-flight acquisition.** *J Comput Assist Tomogr* 1993;17:15–21
30. Parker DL, Yuan C, Blatter DD. **MR angiography by multiple thin slab 3D acquisition.** *Magn Reson Med* 1991;17:434–451
31. Metens T, Rio F, Balériaux D, Roger T, David P, Rodesch G. **Intracranial aneurysms: detection with gadolinium-enhanced dynamic three-dimensional MR angiography: initial results.** *Radiology* 2000;216:39–46
32. Jäger HR, Ellamushi H, Moore EA, Grieve JP, Kitchen ND, Taylor WJ. **Contrast-enhanced MR angiography of intracranial giant aneurysms.** *AJNR Am J Neuroradiol* 2000;21:1900–1907
33. Frayne R, Goodyear BG, Bickhof P, Lauzon ML, Sevick RJ. **Magnetic resonance imaging at 3T esla: challenges and advantages in clinical neurological imaging.** *Invest Radiol* 2003;38:385–402